

EVOLUTIONARY BIOLOGY

Vasopressin-oxytocin–type signaling is ancient and has a conserved water homeostasis role in euryhaline marine planarians

Aoshi Kobayashi¹, Mayuko Hamada¹, Masa-aki Yoshida², Yasuhisa Kobayashi^{1,3}, Naoaki Tsutsui^{1,4}, Toshio Sekiguchi^{5,6}, Yuta Matsukawa¹, Sho Maejima¹, Joseph J. Gingell⁷, Shoko Sekiguchi¹, Ayumu Hamamoto^{1,8}, Debbie L. Hay^{6,9}, John F. Morris¹⁰, Tatsuya Sakamoto¹, Hirota Sakamoto^{1,10*}

Vasopressin/oxytocin (VP/OT)–related peptides are essential for mammalian antidiuresis, sociosexual behavior, and reproduction. However, the evolutionary origin of this peptide system is still uncertain. Here, we identify orthologous genes to those for VP/OT in Platyhelminthes, intertidal planarians that have a simple bilaterian body structure but lack a coelom and body-fluid circulatory system. We report a comprehensive characterization of the neuropeptide derived from this VP/OT-type gene, identifying its functional receptor, and name it the “platytocin” system. Our experiments with these euryhaline planarians, living where environmental salinities fluctuate due to evaporation and rainfall, suggest that platytocin functions as an “antidiuretic hormone” and also organizes diverse actions including reproduction and chemosensory-associated behavior. We propose that bilaterians acquired physiological adaptations to amphibious lives by such regulation of the body fluids. This neuropeptide-secreting system clearly became indispensable for life even without the development of a vascular circulatory system or relevant synapses.

INTRODUCTION

Physiological processes and behavior are controlled and regulated in part by a huge variety of neuronally secreted peptide signaling molecules (neuropeptides) (1–3). Mammalian vasopressin (VP) and oxytocin (OT) are among the most intensively studied and best understood neuropeptides (4). It has very recently been proposed that the VP and OT family of molecules should be referred to as vasotocin based on evolutionary relationships (5). VP and OT are serially homologous; they descended from a single ancestral gene through duplication and subfunctionalization and were originally found based on their peripheral actions as pituitary hormones in mammals where VP acts as an antidiuretic hormone (ADH) and increases blood pressure (2, 6), whereas OT causes uterine contraction in parturition and milk ejection in lactation (1). Both peptides are released, not only into the bloodstream but also into the central nervous system where they have been shown to be important for emotion, bonding, and various sociosexual behaviors in humans and other animals (4, 7).

Phylogenetic analyses of genome/transcriptome sequence data have enabled the discovery of genes encoding VP/OT-type neuropeptides

in many deuterostome phyla (vertebrates and invertebrate chordates, hemichordates, and echinoderms) and protostomes (e.g., arthropods, nematodes, mollusks, and annelids). Thus, the evolutionary origin of this neuropeptide family can be traced back to the bilaterian common ancestor (8–11). VP/OT-type neuropeptides in insects and mollusks have VP-like roles in fluid homeostasis (12, 13), whereas the VP/OT-type neuropeptide in leeches has an OT-like role in reproductive physiology (14). Furthermore, the application of reverse genetic techniques in the nematode *Caenorhabditis elegans* has revealed that VP/OT-type signaling is required for a change in chemotaxis behavior on the basis of prior experience and for normal mating behavior in this species (15, 16), consistent with the actions of VP and OT in mammals (17). However, until now, it has been thought that VP/OT-type signaling has not been studied in planarians, which have a simple bilaterian body structure but lack a coelom and body-fluid circulatory system (8). To provide important new insights into the origin-evolution of this neuropeptide signaling system in the animal kingdom, we here demonstrate the existence of VP/OT-related “platytocin” signaling in two marine planarians, *Stylochoplana pusilla* and *Notocoplana humilis*, and we address the functions of platytocin in these amphibious, euryhaline animals.

RESULTS

Through homology searches, we identified in each planarian species a platytocin gene with similarity to mammalian VP/OT (Fig. 1A and fig. S1). Most amino acid residues of pro-platytocin match the neurohypophyseal peptide motif, including the S–S bond between cysteines, supporting our proposal that platytocin belongs to the VP/OT peptide family (Fig. 1B and fig. S1). In addition, the mature platytocin peptide is identical in the two different species we examined (fig. S1). Phylogenetic analyses of planarian vasotocin precursors indicate that platytocin in the marine planarians is positioned within a clade comprising VP/vasotocin orthologs from other spiralian (fig. S2).

¹Ushimado Marine Institute (UMI), Graduate School of Natural Science and Technology, Okayama University, Ushimado, Setouchi, Okayama 701-4303, Japan. ²Oki Marine Biological Station, Shimane University, 194 Kamo, Okinoshima, Oki, Shimane 685-0024, Japan. ³Laboratory for Aquatic Biology, Department of Fisheries, Faculty of Agriculture, Kindai University, Nakamachi, Nara, Japan. ⁴Department of Marine Bioresources, Faculty of Bioresources, Mie University, Tsu, Mie 514-8507, Japan. ⁵Noto Marine Laboratory, Institute of Nature and Environmental Technology, Division of Marine Environmental Studies, Kanazawa University, Ogi, Noto-cho, Ishikawa 927-0553, Japan. ⁶School of Biological Sciences and Maurice Wilkins Centre for Molecular Biodiscovery, University of Auckland, Auckland, New Zealand. ⁷Vertex Pharmaceuticals (Europe) Ltd., Milton Park, Abingdon OX11 4RW, UK. ⁸Department of Biology, Faculty of Science, Okayama University, 3-1-1 Kita-ku, Tsushimanaka, Okayama 700-8530, Japan. ⁹Department of Pharmacology and Toxicology, University of Otago, Otago, New Zealand. ¹⁰Department of Physiology, Anatomy, and Genetic, Le Gros Clark Building, University of Oxford, South Parks Road, Oxford OX1 3QX, UK. *Corresponding author. Email: hsakamo@okayama-u.ac.jp

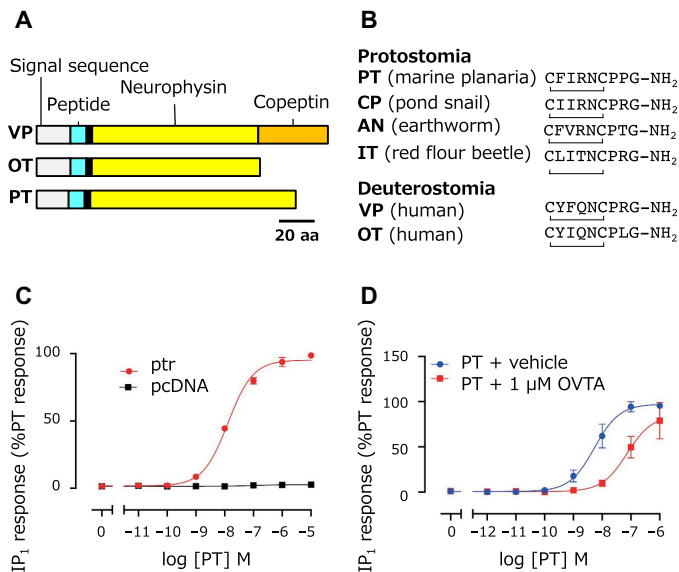


Fig. 1. Platytoxin (PT), a VP/OT-related neuropeptide, signals through a platytoxin receptor (*ptr*). (A) Domain structure/amino acid (aa) sequence of VP, OT, and PT precursors. (B) Amino acid sequence of PT and other VP/OT-type peptides. (C) and (D) Dose-response curves of COS-7 cells transfected with *ptr* when exposed to synthetic PT peptide (C) and OVTA (D), demonstrated by measuring the intracellular IP₁ responses. Error bars in all figures indicate mean \pm SEM ($n = 4$). AN, annetocin; CP, conopressin; IT, inotocin.

We further confirmed their orthologous relationships by reciprocal BLAST best hits between the platytoxin and VP/vasotocin in the bilaterians used in this analysis (fig. S2). In Platyhelminthes, the genome/gene sequences of various species including many parasitic and pathogenic species and model species such as the freshwater planaria *Schmidtea mediterranea* have been published, but our bidirectional BLAST search in public databases (PAA 85176.1, PAA 50340.1, PAA 46766.1, and PAA 87831.1) revealed genes for VP/vasotocin precursors only in the free-living marine flatworm *Macrostomum lignano*, which lives in the intertidal zone (18). Furthermore, our analysis of the transcriptome of *S. pusilla* and *N. humilis* also predicts a G protein-coupled receptor related to vertebrate OT and VP receptors, the platytoxin receptor (*ptr*) gene (fig. S3), although clear orthologous genes for VP/vasotocin receptors were not found in any other Platyhelminthes species including *M. lignano*. We confirmed their orthologous relationships by reciprocal BLAST best hits between the *ptr* genes and human VP receptors and vasotocin receptors in protostomes (fig. S4). To determine whether the *ptr* gene encodes a functional platytoxin receptor (PTR), COS-7 cells transfected with *ptr* expression vector were treated with a synthetic cyclized platytoxin peptide. The cyclized peptide induced accumulation of intracellular myo-inositol 1 phosphate (IP₁) and adenosine 3',5'-monophosphate (cAMP) in a concentration-dependent manner with (mean \pm SEM) pEC₅₀ values of 7.85 ± 0.01 ($n = 4$) and 5.85 ± 0.17 ($n = 4$), respectively (Fig. 1C and fig. S5). We have also identified an antagonist of the platytoxin pathway. The antagonist of the mammalian OT receptor [d(CH₂)₅¹, Tyr(Me)², Thr⁴, Orn⁸, Tyr⁹-NH₂]-vasotocin (OVTA) blocked platytoxin-mediated IP₁ accumulation with a (mean \pm SEM) pA₂ value of 6.99 ± 0.27 ($n = 4$) (Fig. 1D). Although heterologous expression may not capture all native functions, these results suggest that the PTR can contribute to platytoxin-mediated signaling in vivo.

The expression of platytoxin and *ptr* genes was examined by in situ hybridization and with an antiserum raised in chicken against synthetic platytoxin of the marine planarians (Fig. 2 and figs. S6 to S8). Platytoxin precursor transcripts and platytoxin were expressed in two pairs of neurons in the anterior and lateral parts of the cranial ganglion (Fig. 2, A and B, and figs. S7 and S8). Processes of platytoxin neurons extend from the posterior parts from these cell bodies, and some of the processes cross in the midline of the cranial ganglion (Fig. 2B and fig. S8). Immunoelectron microscopy demonstrated that varicosities of these processes contained dense-cored neurosecretory vesicles, the content of which was labeled by immunogold particles (Fig. 2C), demonstrating that platytoxin is a functional secretory neuropeptide in the planarian central nervous system. In addition, smaller electron-lucent vesicles reminiscent of synaptic vesicles could also be seen with the dense-cored vesicles in some of the varicosities (fig. S9). The expression of the putative *ptr* was more widespread and was identified in a number of neurons in the cranial ganglion and in the putative mushroom bodies (19), in cells in the muscular layer of the pharynx, and in interstitial cells scattered in the peripheral tissues, including protonephridial and gonadal regions (Fig. 2, D and E).

Because nanomolar concentrations of platytoxin stimulated intracellular signaling in vitro (Fig. 1C and fig. S5), experiments were designed to test the effects of platytoxin over a similar concentration range in vivo. First, because intertidal planarians would appear to be suitable for examining ADH-like functions of platytoxin, we investigated whether platytoxin regulates water homeostasis in planarians. We used marine planarians, which are not common model organisms, rather than freshwater planarians, because these intertidal planarians, living where the salinities fluctuate considerably due to evaporation and rainfall, are amphibious and euryhaline. As expected, marine planarians can survive in a wide range of salinity concentrations for several days or longer (fig. S10). In hyper-osmotic 70-ppt (parts per thousand) salinity where water absorption is restricted, untreated *S. pusilla* survived for only 1 day, whereas those immersed in 10^{-7} to 10^{-5} M platytoxin survived significantly longer ($P < 0.001$; Fig. 3A and fig. S10); in contrast, those immersed in the PTR blocker OVTA died rapidly ($P < 0.01$; Fig. 3B). In hypo-osmotic 14-ppt salinity, there was no effect of platytoxin on the survival ratio ($P = 0.76$; Fig. 3C). We infer from these observations, from the induced increase in expression of platytoxin in hyper-osmotic salinity ($*P < 0.05$; Fig. 3D), and from the distribution of *ptr* transcript in the protonephridial regions (Fig. 3E) where a classical aquaporin (AQP) gene was also expressed (Fig. 3F and figs. S11 to S13) that platytoxin functions as an “ADH” and increases resistance to hyperosmolality specifically by acting in the protonephridia to cause activation of downstream PTR-mediated mechanisms that induce water absorption (20), presumably via the AQP2 as occurs in mammalian VP systems (Fig. 3G) (21). In addition, the effect of platytoxin on the egg-laying activity in marine planarians was examined (fig. S14). Platytoxin (10^{-5} M) had a stimulatory effect on the induction of egg-laying (fig. S15).

Next, we studied the chemotaxis behavior of *N. humilis* treated with platytoxin. We used *N. humilis* because these planarians are predatory, more active than commensal *S. pusilla*, and are more sensitive to odors derived from its prey, making them more appropriate for experiments of chemotaxis behavior (Fig. 4, A and B, and fig. S16). This experiment used diluted rat blood only as an attractant for fasted planarians. Untreated *N. humilis* showed a

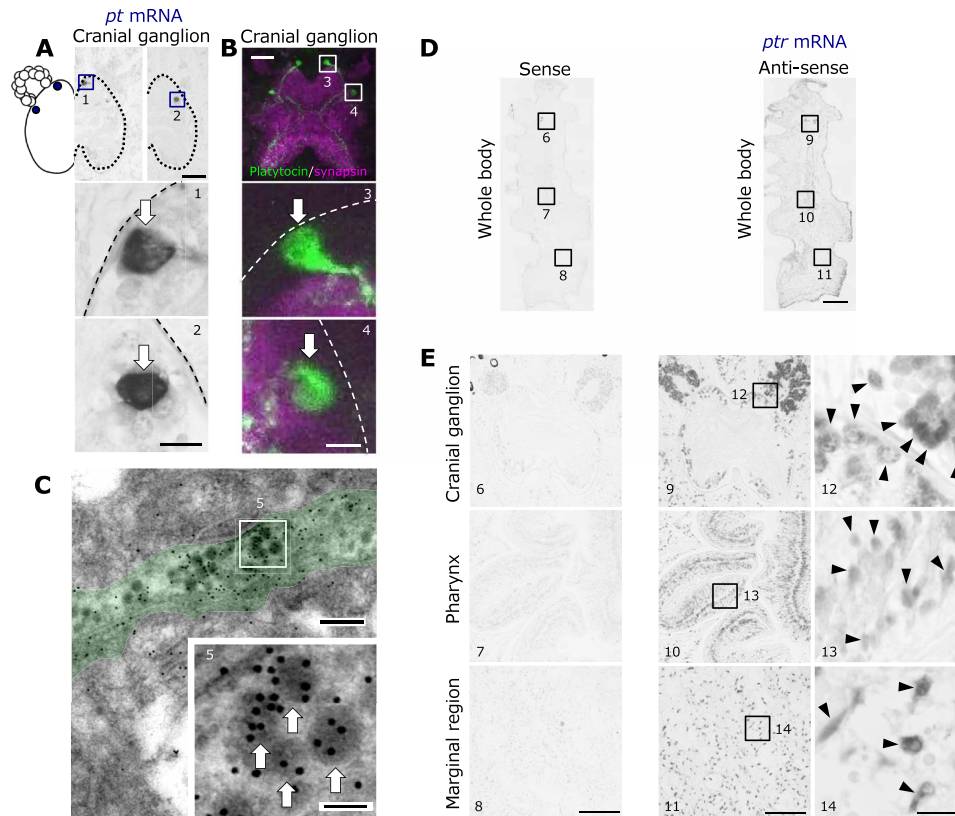


Fig. 2. Platytoxin and a platytoxin receptor (*ptr*) expression patterns. (A) In situ hybridization reveals a pair of platytoxin neurons on either side of the cranial ganglion (white arrows). (B) Immunohistochemistry shows the two neuronal cell bodies (white arrows) and some of their processes. Scale bars, 100 μm in the lower-magnification images and 10 μm in the higher magnification images in (A) and (B). (C) Electron microscopy shows a neuronal process containing a number of platytoxin-immunoreactive dense-cored vesicles. The box shows at higher power the immunogold reactivity of a cluster of five such vesicles (arrows). Scale bars, 200 nm in the lower-magnification image and 50 nm in the higher-magnification image. (D) The whole worm picture for *ptr* expression by in situ hybridization. Scale bar, 1 mm. (E) The *ptr* gene is expressed in a number of neurons in the cranial ganglion and in the putative mushroom bodies, cells in the muscular layer of the pharynx, and interstitial cells scattered in the peripheral tissues including protonephridial and gonadal regions (arrowheads). Scale bars, 100 μm in the lower-magnification images and 10 μm in the higher-magnification images in (E).

marked attraction to the chemosensory cue (rat blood), whereas those immersed in seawater containing 10^{-7} to 10^{-5} M platytoxin showed a significantly reduced attraction (Fig. 4C and fig. S16). Hence, platytoxin interferes with the normal detection of chemosensory cues and/or the subsequent motor responses toward the attractant. We then focused on chemosensory plasticity, which shows that planarians previously exposed to rat blood respond differently to its presence on subsequent exposure. We subjected platytoxin-treated *N. humilis* to a chemotaxis behavior paradigm by using a short-term chemosensory plasticity assay. Chemotaxis toward the attractant (chemosensory cue) in the absence and presence of platytoxin was compared in attractant-naïve planarians and behavioral track-tracing demonstrated the effects of platytoxin on chemotaxis behavior (Fig. 4B). The tracks in Fig. 4B also suggest that the rat blood is not really a “target” and is, instead, just the center of the arena. Planarians treated with platytoxin approached the chemosensory stimulus more slowly than those that were untreated (Fig. 4C). Some animals were pre-exposed to the attractant in the absence of food (as a no-reward stimulus). Although food and the relevant non-nutritious substances might be attractive, platytoxin increases the time it takes *N. humilis* to move toward an attractant such as rat

blood (Fig. 4D and fig. S17). Together, these results indicate that this no-reward response was attenuated in those treated with platytoxin. Platytoxin might affect motor behavior (or possibly some aspect of hunger sensing) in the planarians, causing them to take much longer to reach the rat blood.

DISCUSSION

Here, we report the characterization of VP/OT-type neuropeptide signaling in Platyhelminthes. A VP/OT-related peptide in amphibious, euryhaline planarians regulates body fluid even though these animals have not developed a cardiovascular system. Our experiments with these intertidal planarians, living where environmental salinities fluctuate, demonstrate that platytoxin functions as an “ADH.” Freshwater planarians and parasitic schistosomes that live in stable salinities may have lost platytoxin from their genomes (8, 22). Nematocin functions related to water regulation in the freshwater *C. elegans* were not tested (15, 16), and whether an ADH-like function is an ancestral function has remained uncertain until our study. Our research suggests that platytoxin has an ancient ADH role, which is conserved in both deuterostomes and protostomes, and

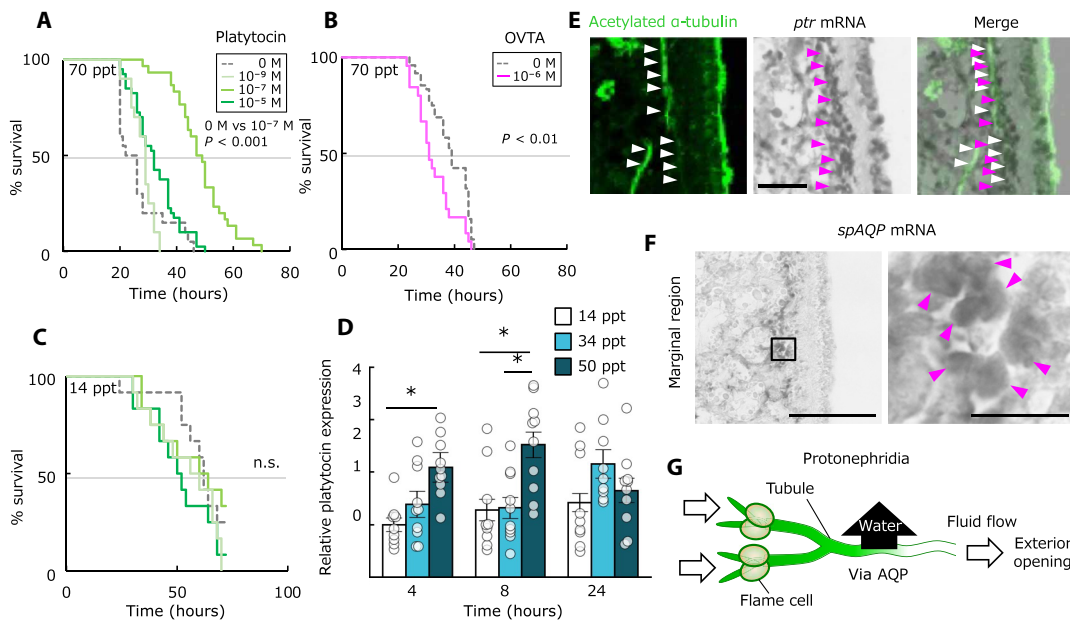


Fig. 3. Platytoxin induces hyperosmolality resistance and egg-laying. (A to C) Survival curves for control [gray dashed line, n = 20 (A), 45 (B), and 12 (C) planarians], 10⁻⁹ M platytoxin-treated [light green, n = 20 (A) and 12 (C) planarians], 10⁻⁷ M platytoxin-treated [green, n = 30 (A) and 12 (C) planarians], 10⁻⁵ M platytoxin-treated [dark green, n = 40 (A) and 12 (C) planarians], and the antagonist of the platytoxin pathway OVTA-treated (magenta, n = 45 planarians) *S. pusilla* in 70-ppt salinity (A and B) or 14-ppt salinity (C). (A) Hyperosmolality (70 ppt) resistance is induced by 10⁻⁷ M platytoxin. (B) Hyperosmolality (70 ppt) resistance is blocked by 10⁻⁶ M OVTA. (C) There was no significant effect of platytoxin on hypoosmolality resistance. Probably because of the effect of high pharmacological dose of platytoxin on the endogenous platytoxin system, 10⁻⁵ M platytoxin has no significant effect on survival. n.s., not significant. (D) Relative platytoxin expressions in animals exposed to 14-ppt salinity (white), 34-ppt salinity (blue), and 50-ppt salinity (dark blue) for 4, 8, and 24 hours. *P < 0.05; error bars indicate SEM (n ≥ 9 planarians; n ≥ 3 independent assays). (E) Acetylated α-tubulin immunohistochemistry shows the protonephridia (white arrowheads). In situ hybridization of serial sections shows the platytoxin receptor (*ptr*) expression (magenta arrowheads). The merged image (right) shows that *ptr* is expressed in the protonephridia. Scale bar, 50 μm. (F) A classical AQP gene (*spAQP*) was also expressed in interstitial cells scattered in the peripheral tissues (magenta arrowheads) including protonephridial (marginal) region. Scale bars, 100 μm, and 10 μm in the enlarged image. (G) Cartoon shows previous segmentation model of the protonephridia (20).

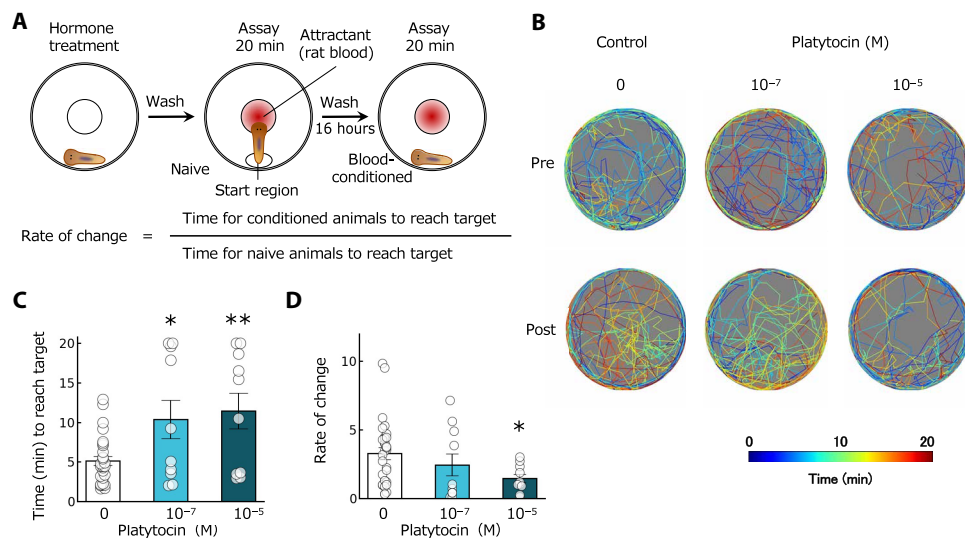


Fig. 4. Platytoxin changes responses to attractive chemosensory cues and chemotaxis behavior. (A) Diagram of the experimental protocol. (B) Behavioral track-tracing illustrated the effects of platytoxin on chemotaxis behavior. (C) Chemotaxis behaviors of *N. humilis*. Planarians were deprived of food for a week before the start of the experiment. Planarians treated with platytoxin approached the chemosensory attractant stimulus (diluted rat blood) more slowly than those that were untreated. (D) Chemosensory plasticity of platytoxin-treated animals. Changes in relative chemotaxis index of animals after pre-exposure to blood (conditioned) or not (naive) are plotted. Statistical significance scores refer to the relative change in behavior of platytoxin-treated animals compared with controls and were based on coefficients of a fitted linear model. All statistical analyses were based on these trajectory data presented in (B). *P < 0.05 and **P < 0.01; error bars indicate SEM (n ≥ 9 planarians; n ≥ 3 independent assays).

therefore demonstrates a hitherto unrecognized evolutionary origin of an antidiuretic control mechanism in the common ancestor of bilaterians. Ancient bilaterians appear to have acquired physiological adaptations to amphibious lives by such regulation of the body fluids, which was regulated by ADH. VP “signals” osmotic water permeability of the renal collecting duct epithelium through regulation of AQP2 through two processes: (i) regulation of AQP2 trafficking to the apical plasma membrane and (ii) regulation of the total amount of the AQP2 protein in the cells. These two modes of water permeability regulation control water excretion in large part (23). Therefore, the transient increase in platytocin expression after exposure to 50-ppt saline appears to be sufficient to maintain fluid homeostasis. It is interesting that the vasotocin ortholog in several ant species (called inotocin) is specifically expressed in only two neurons in the subesophageal zone (24) and also regulates water homeostasis and potentially desiccation resistance (25). Similarly, we found that platytocin in marine planarians is expressed in two pairs of neurons, suggesting that such restricted neuronal expression might be an early feature of the expression of this hormone family.

The broad actions of platytocin not only on osmoregulation but also on reproductive physiology and chemotaxis behavior that we demonstrate could result from the activation of many targets after its secretion into the extracellular fluid surrounding these peptide-secreting neurons and their processes. Hormones are classically defined as molecules circulating via the vascular system, in contrast to the hardwired “synaptic transmission” in the nervous system. There is now very good evidence that not all molecules that we think of as “neurotransmitters” (in particular the central monoamines) are released not only at classic synapses but also from axonal varicosities and dendrites into the extracellular fluid of the central nervous system (17, 26). Therefore, the central (neuro)endocrine system might have arisen when animals first acquired a centralized neural system (27) and an internal body-fluid circulatory system (8, 28). This happened at the divergence of protostomes and deuterostomes more than 700 million years ago, when the bilaterian ancestor animals also became mobile and started to make experience-based decisions. Our results suggest that platytocin is a neuromodulatory molecule in planarians, although they lack a vascular system. Understanding the differences between the evolutionarily ancient diffusion-based “humoral” transmission peptidergic systems and the newer, more rapid synaptic systems using conventional neurotransmitters could shed light on the evolutionary origin of the “synapse system” as a characteristic developed from the peptidergic nerve net of primitive nonbilaterians such as cnidarians (29). Thus, three mechanisms—(i) release of peptide or nonpeptide transmitters into extracellular fluid surrounding neurons, (ii) release of nonpeptide neurotransmitters into specialized synaptic clefts, and (iii) release of peptides and amines from specialized neurosecretory terminals associated with blood vessels in a “neurohemal organ”—now coexist and are complementary in advanced *Animalia*. The platytocin system in the planarians in which both dense-cored platytocin-containing vesicles and clear “synaptic” vesicles are colocalized in neuronal processes represents an important “staging post” in this progression. VP and OT in vertebrates are often/usually thought of as “neuroendocrine hormones.” Their endocrine effects were worked out long before it was recognized that they are also released into the central nervous system from both axons and dendrites of the neurons (30, 31).

The platytocin system in the planarians is, we suggest, an ideal system for studying this aspect of regulatory evolution. Although

the features of the common ancestor of bilaterian “urbilaterian” are still under debate, Xenacoelomorpha, which is considered to be a sister group of Bilateria or Ambulacraria and has a simple morphology with a blind gut with only one ventral opening and a simple central nervous system without a coelom or a circulatory system like that of planarians, indicates possible urbilaterian morphology (32). If urbilaterians had such simple body, platytocin homeostasis, which functions without a circulatory system, provides an important insight into the neuroendocrine system in ancient bilaterians. We propose that, in primitive bilaterians, the central neuropeptide secretory system became essential to allow regulation of the body fluids in conjunction with the emergence of a centralized nervous system even before the development of a vascular circulatory system or conventional synapses.

MATERIALS AND METHODS

Animals

Marine planarians (*S. pusilla* and *N. humilis*) were collected from the Ushimado Coast (Okayama, Japan) at low tide. Planarians were maintained in filtered natural seawater and artificial seawater at approximately 25°C in an aquarium and were fed brine shrimp (nauplii of *Artemia* spp.) for a minimum of 3 weeks with natural photoperiod. We used *S. pusilla* in the osmolality experiments (Fig. 3) because they are suitable for this analysis for the following reason: they live within the shell of the sea snail, *Monodonta confusa*, and are likely exposed to a more variable salinity environment. In contrast, *N. humilis* is more sensitive to odors derived from its prey, making it suitable for experiments of chemotaxis behavior (Fig. 4). The animals used in each experiment were all of comparable size. The Committee for Animal Research, Okayama University, Japan authorized the experimental procedures.

Identification and sequence analysis of genes for platytocin, PTR, and AQP

To find genes for prepro-platytocin, PTR, and AQP in marine planarians, mRNA sequencing was performed. For mRNA sequencing, total RNA was extracted from whole body of adult *S. pusilla* and *N. humilis* by Illustra RNAspin Mini (GE Healthcare, Buckinghamshire, UK). mRNA sequence libraries were made using NEBNext Ultra II FS DNA Library Prep Kit for Illumina (New England BioLabs, MA) as described previously (33). Sequencing was performed using Illumina Miseq platforms with 600-cycle chemistry (2 × 300 base pairs). After preprocessing of raw reads for removal of adaptor sequences and low-quality reads, de novo assembly was conducted using Trinity version 2.6.6 (34). Gene sequences of prepro-platytocin, PTR, and AQP were searched in the assembled transcriptome sequences using Basic Local Alignment Search Tool (BLAST). Their sequences were then confirmed by complementary DNA (cDNA) cloning and Sanger sequencing (GenBank accession number platytocin, *S. pusilla*, LC597866 and *N. humilis*, LC597868; spAQP, *S. pusilla*, LC597870; and ptr, *S. pusilla*, LC597867 and *N. humilis*, LC597869). For cloning, total RNA was extracted from the body of single adult *S. pusilla* and *N. humilis* by Illustra RNAspin Mini (GE Healthcare), and cDNA was synthesized using the SuperScript VILO cDNA Synthesis Kit (Thermo Fisher Scientific, Waltham, MA) as described previously (35). cDNA of the genes for prepro-platytocin, PTR, and spAQP were amplified by polymerase chain reaction (PCR) using AmpliTaq Gold DNA Polymerases

(Thermo Fisher Scientific) with primers 5'-AGATCATCGTCGTTATT-GCCGTCCTG-3' and 5'-CCCAATGCCGTTTACAAATCTGATGG-3' for *platytocin* in *S. pusilla*, 5'-GCCATGAAGGTCATCGTTCTC-3' and 5'-CATTCATGAGGCGATCCAAG-3' for *platytocin* in *N. humilis*, 5'-CCATCGTCGGCAACAGTCTC-3' and 5'-AAGC-GAACAAAGAGGAGAATGGG-3' for *ptr* in *S. pusilla*, 5'-ACCTC-GTTCGCCATGCT-3' and 5'-ACCGAAAAGGCATGGATCAG-3' for *ptr* in *N. humilis*, and 5'-CGCATTCGTACCAGCATCGA-3' and 5'-AGAGAAAAGAACGCGCTGA-3' for *spAQP* in *S. pusilla* and cloned into the pGEM-T easy system (Promega, Madison, WI). We performed 5' and 3' RACE (rapid amplification of cDNA ends) and determined that the PTR transcripts in *S. pusilla* contained full 5' and 3' ends.

Phylogenetic analyses and bidirectional BLAST search were performed to confirm that the platytocin, PTR, and spAQP are orthologs of VP/OT, VP/OT receptors, and spAQP characterized in other animals. In the search for orthologous genes for VP/OT and VP/OT receptor in the other Platyhelminthes, the genes that became bidirectional BLAST best hit to the genes in *Homo sapiens* and *S. pusilla* were searched by BLASTP and TBLASTN. We used National Center for Biotechnology Information nr/nt and WormBase ParaSite (<https://parasite.wormbase.org/index.html>) as databases. Multiple alignments of the amino acid sequences were produced with ClustalX (2.1) with gap trimming (36). Sequences of poor quality that did not well align were deleted using BioEdit (37). Phylogenetic analyses were performed using the neighbor-joining method by ClustalX with the default parameters (1000 bootstrap tests and 111 seeds) and the maximum likelihood (ML) method by RAxML version 8.2.12 (38) with PROTGAMMAAUTO (the best-fitting model). Bootstrap analysis was performed on 100 replicates to estimate the support of the ML topology. Representative phylogenetic trees were drawn by using FigTree (<http://tree.bio.ed.ac.uk/software/figtree/>). SignalP 5.0 was used to predict the signal peptide of platytocin (39). Conformation of PTR as G protein-coupled receptors was predicted by using TMHMM2.0 (40).

Real-time qPCR

The quantification of platytocin in *S. pusilla* was performed using real-time quantitative PCR (qPCR). Total RNA was isolated from whole body using the illustra RNAspin Mini RNA Isolation Kit with ribonuclease-free deoxyribonuclease I (GE Healthcare). Samples were reverse-transcribed from 100 ng of total RNA in a 20- μ l volume using a ReverTra Ace qPCR Master mix kit (TOYOBO, Osaka, Japan). Real-time qPCR was carried out on a C1000TM Thermal Cycler (Bio-Rad Laboratories, Irvine, CA). Reactions were performed in a 20- μ l solution, with 200 nM of each primer, 1 μ l of cDNA (10 ng/ μ l) samples, and SYBR-green master mix (KAPA SYBR FAST qPCR kit, KAPA Bio-systems, Boston, MA) according to the manufacturer's instructions. Assays (in duplicate) were repeated at least twice with the constitutive elongation factors as a normalizing control. Primer pairs are 5'-TTTTTCAGTGCCCCGT-CATGAA-3' and 5'-ATTCGGTCGCAAAGGTTTCCG-3' for platytocin and 5'-GCCATGTGCGTCGAAACTTTC-3' and 5'-CCTCCTTGATAACACCGACAGC-3' for elongation factor. The relative changes in mRNA expression were determined using the $2^{-\Delta\Delta Ct}$ method. Statistical significance was determined using one-way analysis of variance (ANOVA). When significance was found, the post hoc Tukey's test for multiple comparisons was performed.

Synthesis of planarian peptides

Platytocin was synthesized as C-terminally amidated and intramolecular disulfide-bonded form by GL Biochem (Shanghai, China) using solid-phase methods using Fmoc chemistry. Peptides were further purified by reversed-phase high-performance liquid chromatography, and the molecular masses were confirmed using an ultrafleXtreme MALDI TOF (matrix assisted laser desorption/ionization tandem time-of-flight)/TOF mass spectrometer (Bruker Daltonics, MA).

Cell culture and transfection

COS-7 cells were cultured in Dulbecco's modified Eagle's medium (DMEM) supplemented with 8% fetal bovine serum at 37°C in a humidified atmosphere containing 5% CO₂. Cells were plated in 96-well plates at 20,000 cells per well and, 24 hours after seeding, were transfected with pcDNA4.1 inserted by open reading frame sequence of *ptr* using polyethylenamine (41).

IP₁ detection

IP₁ assays were performed using the IP-One Tb kit (Cisbio, Bedford, MA) as described previously (42). COS-7 cells 48 hours after transfection were preincubated for 30 min at 37°C in DMEM containing 0.1% bovine serum albumin (BSA), 0.1% dimethyl sulfoxide, and 50 mM LiCl and then treated for 90 min at 37°C with 50 mM LiCl in the presence or the absence of platytocin in an agonist assay. On the other hand, COS-7 cells were cotreated with platytocin and the mammalian OT receptor blocker OVTA (H-9405, Bachem, Bubendorf, Switzerland) for 90 min at 37°C. After the medium was aspirated, a detection mix containing 14 μ l of buffer, 3 μ l of IP₁-coupled d2 fluorophore, and 3 μ l of Eu-cryptate-conjugated anti-IP₁ monoclonal antibody was added to the samples. After incubation at room temperature for 1 hour with shaking, 15- μ l aliquots of the sample were transferred to a 384-well white opti-plate (Perkin Elmer, Waltham, MA). Time-resolved fluorescence was measured by using an EnSpire plate reader (Perkin Elmer). The concentration of IP₁ in each sample was calculated from a standard curve in each assay. Assays were performed with four independent samples. The potency of agonist (pEC₅₀) and antagonist (pA₂) was calculated by three-parameter nonlinear regression curve fitting and global Schild analysis, with a slope of 1 using Prism 7.0c GraphPad, respectively (GraphPad Software, La Jolla, CA).

cAMP detection

The concentration of cAMP in transfected COS-7 cells was measured using a LANCE cAMP assay kit (Perkin Elmer) as described previously (43). In brief, cells were preincubated for 30 min with 1 mM 3-isobutyl-1-methylxanthine diluted in serum-free DMEM containing 0.1% BSA and then treated for 15 min at 37°C with platytocin peptide. The medium was removed and changed to 50 μ l of absolute ice-cold ethanol. After ethanol was evaporated, 50 μ l of LANCE detection buffer, including 50 mM Hepes (pH 7.4), 10 mM CaCl₂, and 0.35% Triton X-100, was added to wells and incubated at room temperature for 15 min with gently shaking. We transferred 5 μ l of cell lysates to each well of a 384-well white opti-plate (Perkin Elmer), added 5 μ l of anti-cAMP antibody diluted in detection buffer to each well, and incubated the plate in the dark for 30 min at room temperature. Next, 10 μ l of the detection mix was added to each well, and the plate was incubated in the dark for 4 hours. Time-resolved fluorescence was measured using an EnSpire plate reader

(Perkin Elmer). The concentration of cAMP was calculated from a standard curve prepared in each assay. Assays were performed with four independent biological samples, and the results were analyzed by nonlinear regression using Prism 7.0c GraphPad.

Tissue preparation

For immunohistochemistry and in situ hybridization, specimens were fixed in 4% paraformaldehyde in 0.1 M phosphate buffer (PB; pH 7.4) overnight at 4°C. Following fixation, preparations were dehydrated through graded ethanol concentrations, cleared in lemosol, embedded in paraffin wax, and sectioned on an HM 325 microtome (Leica, Wetzlar, Germany). Horizontal sections (7 µm in thickness) were mounted on glass slides (Matsunami Glass, Osaka, Japan).

In situ hybridization

Expression patterns of genes for platytocin, PTR, and spAQP were detected with digoxigenin (DIG)-labeled RNA probes. DIG-labeled probes were synthesized by DIG-labeling mix and SP6/T7 RNA polymerases according to the manufacturer's instructions (Merck, Darmstadt, Germany). Sense probe targeting the same sequences as the antisense probe was used as a negative control. Primers used for amplification of the target regions are the same as for cDNA cloning. Sections were immersed in xylene three times for 5 min each and then in a decreasing series of ethanol concentrations and lastly washed with a solution (TNT) containing 0.1 M tris-HCl (pH 7.5), 0.15 M NaCl, and 0.05% Tween 20 and then incubated in a Proteinase K solution for 15 min at 38°C. Sections were then rinsed with TNT and acetylated with 0.25% acetic anhydride in 0.1 M triethanolamine. Following acetylation, sections were again rinsed with TNT and incubated in hybridization buffer for 30 min at 60°C and DIG-labeled RNA probes in hybridization buffer overnight at 60°C. Sections were washed with 50% formamide in 0.3 M sodium citrate and 3 M NaCl (SSC) decreasing series of SSC for 30 min at 60°C each. Sections were rinsed with 0.1 M tris-HCl (pH 7.5) and 0.17 M NaCl and 0.01% Tween 20 (wash buffer1) and nonspecific binding components were blocked with 1.5% blocking reagent (Merck) in 0.1 M tris-HCl (pH 7.5) and 0.17 M NaCl for 1 hour, followed by incubation in the sheep anti-DIG Fab fragment antibodies conjugated to alkaline phosphatase in wash buffer1 [1:1000 dilution, Merck; research resource identifier (RRID): AB_2734716] for 2 hours at room temperature. Sections were rinsed with wash buffer1 three times for 5 min each and incubated in 0.1 M tris-HCl (pH 9.5) and 0.1 M NaCl for 5 min. Hybridization signal was visualized using NBT/BCIP (nitro-blue tetrazolium chloride/5-bromo-4-chloro-3'-indolyl phosphate p-toluidine salt) staining solution (Merck). Images were obtained using an FSX100 (Olympus, Tokyo, Japan) microscope.

Immunohistochemistry and immunofluorescence

For immunoperoxidase histochemistry, sections were soaked in xylene three times for 5 min each to remove wax, then in a decreasing series of ethanol concentrations, washed with phosphate-buffered saline (PBS) containing 0.1% Triton X-100 (PBST), and then incubated in a solution of 0.3% H₂O₂ in absolute methanol for 20 min to eliminate endogenous peroxidase activity. After nonspecific binding components were blocked with 1% normal goat serum and 1% bovine serum albumin in PBS containing 0.1% Triton X-100 (TNGS) for 1 hour at room temperature, sections were incubated with the primary chicken antiserum against platytocin (1:50,000 dilution,

developed in our laboratory; RRID: AB_2885040) for 1 hour at room temperature and overnight at 4°C and then incubated in a solution of biotinylated anti-chicken immunoglobulin G (IgG) raised in goats (1:1000 dilution, Maravai LifeSciences, San Diego, CA) in TNGS. Immunopositive products were detected with a VECTASTAIN ABC Rabbit IgG Kit (Vector Laboratories, Burlingame, CA), followed by diaminobenzidine development, as described previously (44). Images were obtained using an FSX100 microscope.

For immunofluorescence, sections were soaked in xylene three times for 5 min each and then in a decreasing series of ethanol concentrations and washed with PBST. After nonspecific binding components were blocked with TNGS for 1 hour at room temperature, sections were incubated with the primary chicken antiserum against platytocin (1:50,000 dilution) or rabbit antiserum against acetyl- α -tubulin (1:250 dilution, Santa Cruz Biotechnology, Dallas, TX; RRID: AB_628409) for 1 hour at room temperature and overnight at 4°C. Alexa Fluor 488-labeled anti-chicken IgG and Alexa Fluor 488-labeled anti-rabbit IgG (Molecular Probes) at a 1:1000 dilution were used for detection. Immunoreacted specimens were rinsed with PBS, mounted on glass slides, and covered with cover glass. Images were obtained using an FV1000 (Olympus) confocal laser scanning microscope.

Whole mount immunofluorescence

Planarians were soaked in 7.5% *N*-acetyl-L-cysteine in PBS for 10 min to remove the mucus layer surrounding the animals and fixed in 4% paraformaldehyde in 0.1 M PB (pH 7.4) overnight at 4°C. Specimens were dehydrated in 50% methanol in PBST and absolute methanol for 30 min each at 4°C. Following dehydration, specimens were incubated overnight with 6% H₂O₂ in absolute methanol at room temperature to remove pigment. Specimens were rehydrated in absolute methanol and 50% methanol in PBST for 30 min at 4°C and washed with PBST for 30 min. After nonspecific binding components were blocked with TNGS for 2 hours at room temperature, specimens were incubated with the primary chicken antiserum against platytocin (1:50,000 dilution) and 3C11 (mouse antiserum against synapsin) (1:300 dilution, Developmental Studies Hybridoma Bank, Iowa City, IA; RRID: AB_528479) overnight at room temperature. Specimens were next washed with PBST for 30 min and incubated in TNGS for 2 hours at room temperature. Alexa Fluor 488-labeled anti-chicken IgG and Alexa Fluor 546-labeled anti-mouse IgG (Molecular Probes) were all used for detection at a 1:1000 dilution. Immunoreacted specimens were rinsed with PBS, and the cranial ganglia were isolated from the animals, mounted on glass slides, and covered with cover glass. Images were obtained using an FV1000 confocal laser scanning biological microscope.

Immunolectron microscopy

Marine planarians (*S. pusilla*) were fixed with 4% paraformaldehyde and 0.1% glutaraldehyde in PBS overnight at 4°C. Preparations were dehydrated through increasing concentrations of methanol, embedded in LR Gold resin (Electron Microscopy Sciences, PA), and polymerized under ultraviolet lamps at -20°C for 24 hours as described previously (45). Ultrathin sections (70 nm in thickness) were collected on nickel grids coated with a collodion film, rinsed with PBS several times, and then incubated with 2% normal goat serum and 2% BSA in 50 mM tris(hydroxymethyl)-aminomethane-buffered saline (pH 8.2) for 30 min to block nonspecific binding. The sections were then incubated with a 1:500 dilution of the chicken polyclonal

antiserum against platytocin for 1 hour at room temperature. The sections were washed with PBS and then incubated with a 1:50 dilution of a goat antibody against chicken IgG conjugated to 10-nm gold particles (Abcam, Cambridge, UK) for 1 hour at room temperature. Last, the sections were contrasted with uranyl acetate and lead citrate and viewed using an H-7650 (Hitachi, Tokyo, Japan) electron microscope operated at 80 kV.

Survival rate after salinity exposure

We chose different salinity values to simulate increases in salinity at low tide on hot sunny days due to evaporation (50 and 70 ppt) and reduced salinity under conditions of increased freshwater input (e.g., the salinity levels can fall rapidly during heavy rainfall runoff; 7 to 17 ppt), as well as the normal salinity level (34 ppt, considered here as control conditions), these being the salinities that these planarians encounter in their natural environment. Each *S. pusilla* was placed in the individual well (at least 10 per treatment) of 24-well plates (wells 16 × 10 mm; total volume, 2 ml) with replacement from 34-ppt seawater to the respective salinity solution. The volume in each well was standardized to 300 μ l. The animals were exposed to these environments for 3 days except for the gene expression analyses (2 days). All analyses were carried out in artificial seawater at 25°C. Salinity was checked with a refractometer. Survival of planarians (motile/active or immotile/dead) was checked every 1 hour after the immersion exposure.

To examine the effects on survival of treatment with platytocin or OVTA, which we identified as a specific antagonist of the platytocin pathway, planarians were immersed in 34-ppt seawater of 0 (control), 10^{-9} , 10^{-7} , or 10^{-5} M platytocin or OVTA. The doses were chosen on the basis of the results of our preliminary studies and effective physiological doses (13, 46). On the day of use, an aliquot of each agent was diluted in the 34-ppt seawater. After 24 hours of treatment ($n = 12$ to 40 planarians in each group), each animal was placed in the well containing 14- and 70-ppt seawater. These salinities were chosen on the basis of the range of salinity tolerance for this species (fig. S10). Exposures were replicated at least twice. Statistical significance was determined using the log-rank test and Holm's test for multiple comparisons.

Oviposition

Mature planarians (*N. humilis*) were stimulated by three different doses of platytocin (10^{-9} , 10^{-7} , or 10^{-5} M) dissolved in seawater in the same manner as described above. The behaviors of animals in the wells were observed and recorded by using a digital camera. The latent period was defined as the time required for induction of egg-laying after treatment. Experiments were carried out during the spawning season (June–July). Statistical significance was determined using one-way ANOVA. When significance was found, the post hoc Dunnett's test for multiple comparisons was performed.

Chemotaxis and chemosensory plasticity

Chemotaxis and chemosensory plasticity were assessed as illustrated in Fig. 4A and fig. S16. Assays were performed in petri dish chambers (Falcon X plate, Becton Dickinson, Franklin Lakes, NJ). To obtain reproducible assay results, rat blood was divided into small stocks and frozen until use as the chemosensory chemoattractant in the absence of food. All planarians were fasted for a week before the behavioral tests. Twenty microliters of the 10-fold diluted blood was placed in the center of the chamber. Assay chambers were prepared

freshly in each time. Planarians (*N. humilis*) treated with platytocin for 24 hours (as in survival after salinity exposure) were placed at the edge of the chamber (Fig. 4A). The behavior of each animal was captured using an HDR-CX680/W (Sony, Tokyo, Japan) video recorder placed above the container, and the time to reach the target region was determined as indicated in fig. S16. The behavior of planarians in platytocin-treated groups was compared with that of the control (0 M platytocin) group always performed on the same day. An animal for chemosensory plasticity assays was pre-exposed to the blood (blood-conditioned animals) or not pre-exposed (naive animals) and tested for 20 min for the same chemotaxis. The time to reach the target was determined. The track-tracing of moving planarians was analyzed with a computer, ImageJ, and Python software.

Statistical significance was determined using one-way ANOVA. When significance was found, the post hoc Dunnett's test for multiple comparisons was performed. All chemotaxis assays were conducted at least three times and on at least two separate days in a dark room with only a red light of a wavelength that cannot be sensed by planarians (47, 48).

SUPPLEMENTARY MATERIALS

Supplementary material for this article is available at <https://science.org/doi/10.1126/sciadv.abk0331>

[View/request a protocol for this paper from Bio-protocol.](#)

REFERENCES AND NOTES

- M. S. Soloff, M. Alexandrova, M. J. Fernstrom, Oxytocin receptors: Triggers for parturition and lactation? *Science* **204**, 1313–1315 (1979).
- M. Birnbaumer, A. Seibold, S. Gilbert, M. Ishido, C. Barberis, A. Antaramian, P. Brabet, W. Rosenthal, Molecular cloning of the receptor for human antidiuretic hormone. *Nature* **357**, 333–335 (1992).
- M. Schumacher, H. Coirini, D. W. Pfaff, B. S. McEwen, Behavioral effects of progesterone associated with rapid modulation of oxytocin receptors. *Science* **250**, 691–694 (1990).
- Z. R. Donaldson, L. J. Young, Oxytocin, vasopressin, and the neurogenetics of sociality. *Science* **322**, 900–904 (2008).
- C. Theofanopoulou, G. Gedman, J. A. Cahill, C. Boeckx, E. D. Jarvis, Universal nomenclature for oxytocin-vasotocin ligand and receptor families. *Nature* **592**, 747–755 (2021).
- W. Rosenthal, A. Seibold, A. Antaramian, M. Lonergan, M. F. Arthus, G. N. Hendy, M. Birnbaumer, D. G. Bichet, Molecular identification of the gene responsible for congenital nephrogenic diabetes insipidus. *Nature* **359**, 233–235 (1992).
- H. Walum, L. J. Young, The neural mechanisms and circuitry of the pair bond. *Nat. Rev. Neurosci.* **19**, 643–654 (2018).
- E. A. Odekunle, M. R. Elphick, Comparative and evolutionary physiology of vasopressin/oxytocin-type neuropeptide signaling in invertebrates. *Front. Endocrinol.* **11**, 225 (2020).
- M. R. Elphick, O. Mirabeau, D. Larhammar, Evolution of neuropeptide signalling systems. *J. Exp. Biol.* **221**, jeb151092 (2018).
- O. Mirabeau, J. S. Joly, Molecular evolution of peptidergic signaling systems in bilaterians. *Proc. Natl. Acad. Sci. U.S.A.* **110**, E2028–E2037 (2013).
- G. Jékely, Global view of the evolution and diversity of metazoan neuropeptide signaling. *Proc. Natl. Acad. Sci. U.S.A.* **110**, 8702–8707 (2013).
- M. J. Aikins, D. A. Schooley, K. Begum, M. Detheux, R. W. Beeman, Y. Park, Vasopressin-like peptide and its receptor function in an indirect diuretic signaling pathway in the red flour beetle. *Insect Biochem. Mol. Biol.* **38**, 740–748 (2008).
- T. Sakamoto, S. Ogawa, Y. Nishiyama, C. Akada, H. Takahashi, T. Watanabe, H. Minakata, H. Sakamoto, Osmotic/ionic status of body fluids in the euryhaline cephalopod suggest possible parallel evolution of osmoregulation. *Sci. Rep.* **5**, 14469 (2015).
- T. Oumi, K. Ukena, O. Matsushima, T. Ikeda, T. Fujita, H. Minakata, K. Nomoto, Annelid oxytocin-related peptide, induces egg-laying behavior in the earthworm, *Eisenia foetida*. *J. Exp. Zool.* **276**, 151–156 (1996).
- J. L. Garrison, E. Z. Macosko, S. Bernstein, N. Pokala, D. R. Albrecht, C. I. Bargmann, Oxytocin/vasopressin-related peptides have an ancient role in reproductive behavior. *Science* **338**, 540–543 (2012).
- I. Beets, T. Janssen, E. Meelkop, L. Temmerman, N. Suetens, S. Rademakers, G. Jansen, L. Schoofs, Vasopressin/oxytocin-related signaling regulates gustatory associative learning in *C. elegans*. *Science* **338**, 543–545 (2012).

17. Z. V. Johnson, L. J. Young, Oxytocin and vasopressin neural networks: Implications for social behavioral diversity and translational neuroscience. *Neurosci. Biobehav. Rev.* **76**, 87–98 (2017).
18. J. Wudarski, B. Egger, S. A. Ramm, L. Schärer, P. Ladurner, K. S. Zadesenets, N. B. Rubtsov, S. Mouton, E. Berezikov, The free-living flatworm *Macrostomum lignano*. *EvoDevo* **11**, 5 (2020).
19. G. H. Wolff, N. J. Strausfeld, Genealogical correspondence of mushroom bodies across invertebrate phyla. *Curr. Biol.* **25**, 38–44 (2015).
20. H. Thi-Kim Vu, J. C. Rink, S. A. McKinney, M. McClain, N. Lakshmanaperumal, R. Alexander, A. Sánchez Alvarado, Stem cells and fluid flow drive cyst formation in an invertebrate excretory organ. *eLife* **4**, e07405 (2015).
21. K. Takata, T. Matsuzaki, Y. Tajika, A. Ablimit, T. Hasegawa, Localization and trafficking of aquaporin 2 in the kidney. *Histochem. Cell Biol.* **130**, 197–209 (2008).
22. M. A. Lockard, M. S. Ebert, C. I. Bargmann, Oxytocin mediated behavior in invertebrates: An evolutionary perspective. *Dev. Neurobiol.* **77**, 128–142 (2017).
23. J. L. Wilson, C. A. Miranda, M. A. Knepper, Vasopressin and the regulation of aquaporin-2. *Clin. Exp. Nephrol.* **17**, 751–764 (2013).
24. I. Fetter-Pruneda, T. Hart, Y. Ulrich, A. Gal, P. R. Oxley, L. Olivos-Cisneros, M. S. Ebert, M. A. Kazmi, J. L. Garrison, C. I. Bargmann, D. J. C. Kronauer, An oxytocin/vasopressin-related neuropeptide modulates social foraging behavior in the clonal raider ant. *PLoS Biol.* **19**, e3001305 (2021).
25. A. Koto, N. Motoyama, H. Tahara, S. McGregor, M. Moriyama, T. Okabe, M. Miura, L. Keller, Oxytocin/vasopressin-like peptide inotocin regulates cuticular hydrocarbon synthesis and water balancing in ants. *Proc. Natl. Acad. Sci. U.S.A.* **116**, 5597–5606 (2019).
26. T. Oti, K. Satoh, D. Uta, J. Nagafuchi, S. Tateishi, R. Ueda, K. Takanami, L. J. Young, A. Galione, J. F. Morris, T. Sakamoto, Oxytocin influences male sexual activity via non-synaptic axonal release in the spinal cord. *Curr. Biol.* **31**, 103–114.e5 (2021).
27. C. L. Keenan, R. Coss, H. Koopowitz, Cytoarchitecture of primitive brains: Golgi studies in flatworms. *J. Comp. Neurol.* **195**, 697–716 (1981).
28. P. Heger, W. Zheng, A. Rottmann, K. A. Panfilio, T. Wiehe, The genetic factors of bilaterian evolution. *eLife* **9**, e45530 (2020).
29. J. A. Westfall, S. Yamataka, P. D. Enos, Ultrastructural evidence of polarized synapses in the nerve net of *Hydra*. *J. Cell Biol.* **51**, 318–323 (1971).
30. M. Ludwig, G. Leng, Dendritic peptide release and peptide-dependent behaviours. *Nat. Rev. Neurosci.* **7**, 126–136 (2006).
31. J. Morris, in *Neurosecretion: Secretory Mechanisms*, G. Lemons, J. R. Dayanithi, Ed. (Springer Nature Switzerland, 2020), vol. 8, chap. 5, pp. 81–102.
32. A. Hejnol, M. Q. Martindale, Acoel development supports a simple planula-like urbilaterian. *Philos. Trans. R. Soc. Lond. Ser. B Biol. Sci.* **363**, 1493–1501 (2008).
33. T. Oti, K. Takanami, S. Ito, T. Ueda, K. I. Matsuda, M. Kawata, J. Soh, O. Ukimura, T. Sakamoto, H. Sakamoto, Effects of sex steroids on the spinal gastrin-releasing peptide system controlling male sexual function in rats. *Endocrinology* **159**, 1886–1896 (2018).
34. M. G. Grabherr, B. J. Haas, M. Yassour, J. Z. Levin, D. A. Thompson, I. Amit, X. Adiconis, L. Fan, R. Raychowdhury, Q. Zeng, Z. Chen, E. Mauceli, N. Hacohen, A. Gnirke, N. Rhind, F. di Palma, B. W. Birren, C. Nusbaum, K. Lindblad-Toh, N. Friedman, A. Regev, Full-length transcriptome assembly from RNA-Seq data without a reference genome. *Nat. Biotechnol.* **29**, 644–652 (2011).
35. K. Tamura, Y. Kobayashi, A. Hirooka, K. Takanami, T. Oti, T. Jogahara, S. I. Oda, T. Sakamoto, H. Sakamoto, Identification of the sexually dimorphic gastrin-releasing peptide system in the lumbosacral spinal cord that controls male reproductive function in the mouse and Asian house musk shrew (*Suncus murinus*). *J. Comp. Neurol.* **525**, 1586–1598 (2017).
36. M. A. Larkin, G. Blackshields, N. P. Brown, R. Chenna, P. A. McGettigan, H. McWilliam, F. Valentin, I. M. Wallace, A. Wilm, R. Lopez, J. D. Thompson, T. J. Gibson, D. G. Higgins, Clustal W and CLUSTAL X version 2.0. *Bioinformatics* **23**, 2947–2948 (2007).
37. Hall, BioEdit: A user-friendly biological sequence alignment editor and analysis program for Windows 95/98/NT. *Nucleic Acids Symp. Ser.* **41**, 95–98 (1999).
38. A. Stamatakis, RAxML version 8: A tool for phylogenetic analysis and post-analysis of large phylogenies. *Bioinformatics* **30**, 1312–1313 (2014).
39. J. J. A. Armenteros, K. D. Tsirigos, C. K. Sønderby, T. N. Petersen, O. Winther, S. Brunak, G. von Heijne, H. Nielsen, SignalP 5.0 improves signal peptide predictions using deep neural networks. *Nat. Biotechnol.* **37**, 420–423 (2019).
40. A. Krogh, B. Larsson, G. von Heijne, E. L. Sonnhammer, Predicting transmembrane protein topology with a hidden Markov model: Application to complete genomes. *J. Mol. Biol.* **305**, 567–580 (2001).
41. R. J. Bailey, D. L. Hay, Pharmacology of the human CGRP1 receptor in Cos 7 cells. *Peptides* **27**, 1367–1375 (2006).
42. R. L. Bower, L. Yule, T. A. Rees, G. Deganutti, E. R. Hendrikse, P. W. R. Harris, R. Kowalczyk, Z. Ridgway, A. G. Wong, K. Swierkula, D. P. Raleigh, A. A. Pioszak, M. A. Brimble, C. A. Reynolds, C. S. Walker, D. L. Hay, Molecular signature for receptor engagement in the metabolic peptide hormone amylin. *ACS Pharmacol. Transl. Sci.* **1**, 32–49 (2018).
43. M. J. Woolley, C. A. Reynolds, J. Simms, C. S. Walker, J. C. Mobarec, M. L. Garelja, A. C. Conner, D. R. Poyner, D. L. Hay, Receptor activity-modifying protein dependent and independent activation mechanisms in the coupling of calcitonin gene-related peptide and adrenomedullin receptors to Gs. *Biochem. Pharmacol.* **142**, 96–110 (2017).
44. H. Sakamoto, K. I. Matsuda, D. G. Zuloaga, H. Hongu, E. Wada, K. Wada, C. L. Jordan, S. M. Breedlove, M. Kawata, Sexually dimorphic gastrin releasing peptide system in the spinal cord controls male reproductive functions. *Nat. Neurosci.* **11**, 634–636 (2008).
45. K. Satoh, T. Oti, A. Katoh, Y. Ueta, J. F. Morris, T. Sakamoto, H. Sakamoto, In vivo processing and release into the circulation of GFP fusion protein in arginine vasopressin enhanced GFP transgenic rats: Response to osmotic stimulation. *FEBS J.* **282**, 2488–2499 (2015).
46. E. A. Odekunle, D. C. Semmens, N. Martyniuk, A. B. Tinoco, A. K. Garewal, R. R. Patel, L. M. Bloway, M. Zandawala, J. Delroisse, S. E. Slade, J. H. Scrivens, M. Egertová, M. R. Elphick, Ancient role of vasopressin/oxytocin-type neuropeptides as regulators of feeding revealed in an echinoderm. *BMC Biol.* **17**, 60 (2019).
47. T. R. Paskin, J. Jellies, J. Bacher, W. S. Beane, Planarian phototactic assay reveals differential behavioral responses based on wavelength. *PLoS ONE* **9**, e114708 (2014).
48. Y. Akiyama, K. Agata, T. Inoue, Coordination between binocular field and spontaneous self-motion specifies the efficiency of planarians' photo-response orientation behavior. *Commun. Biol.* **1**, 148 (2018).

Acknowledgments: We thank D. Kurokawa and N. Satoh for technical support and critical discussion. **Funding:** This work was supported by Grants-in-Aid for Scientific Research from the Japan Society for the Promotion of Science (JSPS) KAKENHI [to H.S., 15K15202, 15H05724, 15KK025708, and 16H06280; and to T.Sa., 21H02520], by Grant-in-Aid for Scientific Research on Innovative Areas “Singularity Biology (No. 8007)” of MEXT, Japan (to T.Sa., 21H00428), by the Research Grant from the Suzuken Memorial Foundation, Japan (to H.S., 19-085), and by the Japan Agency for Medical Research and Development (AMED) (to H.S., 961149). **Author contributions:** A.K., M.H., M.-a.Y., Y.K., N.T., and S.S. performed molecular biological experiments. T.Se., J.J.G., and D.L.H. performed biochemical experiments. A.K., Y.M., and A.H. performed physiological experiments. S.M., J.F.M., and H.S. performed immunoelectron microscopy analyses. T.Sa. and H.S. wrote the paper with assistance from J.F.M. All authors had full access to all the data in the study and take responsibility for the integrity of the data and the accuracy of the data analysis. The whole study was supervised by H.S. **Competing interests:** The authors declare that they have no competing interests. **Data and materials availability:** All data needed to evaluate the conclusions in the paper are present in the paper and/or the Supplementary Materials.

Submitted 17 June 2021

Accepted 11 January 2022

Published 4 March 2022

10.1126/sciadv.abk0331

Vasopressin-oxytocin–type signaling is ancient and has a conserved water homeostasis role in euryhaline marine planarians

Aoshi KobayashiMayuko HamadaMasa-aki YoshidaYasuhisa KobayashiNaoaki TsutsuiToshio SekiguchiYuta MatsukawaSho MaejimaJoseph J. GingellShoko SekiguchiAyumu HamamotoDebbie L. HayJohn F. MorrisTatsuya SakamotoHirota Sakamoto

Sci. Adv., 8 (9), eabk0331. • DOI: 10.1126/sciadv.abk0331

View the article online

<https://www.science.org/doi/10.1126/sciadv.abk0331>

Permissions

<https://www.science.org/help/reprints-and-permissions>

Use of this article is subject to the [Terms of service](#)

Science Advances (ISSN) is published by the American Association for the Advancement of Science. 1200 New York Avenue NW, Washington, DC 20005. The title *Science Advances* is a registered trademark of AAAS.
Copyright © 2022 The Authors, some rights reserved; exclusive licensee American Association for the Advancement of Science. No claim to original U.S. Government Works. Distributed under a Creative Commons Attribution NonCommercial License 4.0 (CC BY-NC).